ELEVENTH EUROPEAN ROTORCRAFT FORUM

Paper No 80

ON THE ANALYSIS OF HELICOPTER FLIGHT DYNAMICS DURING MANOEUVRES

S.S. Houston

Flight Research Division
Royal Aircraft Establishment
BEDFORD MK41 6AE, UK

10-13 September 1985
LONDON, England

THE CITY UNIVERSITY, LONDON EC1V OHB, ENGLAND

ON THE ANALYSIS OF HELICOPTER FLIGHT DYNAMICS DURING MANOEUVRES

S.S. Houston

Flight Research Division
Royal Aircraft Establishment
BEDFORD MK41 6AE, England

ABSTRACT

The short period longitudinal dynamics of a typical single main rotor helicopter in manoeuvring flight are examined in detail. Short term longitudinal motion is shown to be more complex in nature in high bank angle turns than in level flight. As a result, the conventional short period mode approximation is inadequate for predicting stability and response characteristics, although it does predict general trends with increases in bank angle. By qualitatively considering the defining conditions for valid weakly coupled systems analysis, it is argued that this is due to increased coupling which is strong, rather than weak. A novel methodology is described that offers a useful means of quantifying cross coupling, highlighting important derivatives and obtaining rational approximations for the short period mode. Analysis of flight data supports, but does not entirely confirm, the presence of short period pitch - sideslip cross coupling (predicted analytically), or of any associated compensatory pilot workload.

1 INTRODUCTION

The need to study the flight dynamic characteristics of the helicopter in manoeuvres arises because of the requirement to operate close to the edge of the manoeuvre envelope. Combat helicopter pilots, in particular, enhance survivability by flying nap-of-the-earth, but this in turn can involve severe manoeuvring to avoid the very obstacles that the pilot is using for concealment. Applying mathematical models based on level flight to the analysis of manoeuvring flight is fraught with pitfalls, because of the considerable changes in the response modes that occur when manoeuvring. Previous theoretical research in this area appears limited[1,2], although some trends in mode frequency, damping and content have been identified, and in Ref 2 the authors examine the effects of kinematic, inertial and aerodynamic derivatives on the stability of the helicopter. In this paper, the stability of the helicopter in steady coordinated turns is examined, with a view to isolating the features associated with manoeuvring flight that change the helicopter's response modes. These manoeuvres possess several interesting features with regard to the short term longitudinal response characteristics, which are examined in detail because of their importance to handling qualities. The modes themselves change considerably with bank angle. The traditional pitch-heave approximation used to highlight the parameters influencing short period stability progressively breaks down with increasing bank angle, indicating cross coupling of increasing severity in the vehicle's response. By contrast, a somewhat perplexing result is that the predicted response to control inputs using the approximate method is generally accurate enough to assess some features affecting handling

qualities. This paper addresses these aspects in the context of the effect of manoeuvring on handling qualities, and examines the level of approximation necessary to adequately represent both modal characteristics, and the nature of the control responses. The analysis presented in the paper is based on results from a single helicopter design at a limited number of mid-speed-range flight conditions. As such, they serve mainly to illustrate the scope of the problem, rather than to establish trends of a more general nature.

2 THE HELICOPTER IN TURNING FLIGHT

2.1 Definition of turn parameters

When analysing the flight dynamics of helicopters in manoeuvres, it becomes pertinent to question what physical quantities the terms "bank angle" (ϕ) and "load factor" (n) represent. The equation normally used to relate these two quantities is given by,

$$n = \frac{1}{\cos\phi} \tag{1}$$

The error involved in this relationship was observed in Ref 3 and later Chen and Jeske[4], in a detailed analytical study of helicopter kinematics in manoeuvring flight, pointed out that this is probably due to the fact that for the conventional single main rotor helicopter, the fuselage roll attitude and the thrust vector tilt are generally different. The definition of "normal acceleration" given in Ref 4,

$$n_t = \left(1 + \left(\frac{\omega_t V_f}{g}\right)^2\right)^{\frac{1}{2}} \cos\gamma \tag{2}$$

is used in this paper to define the load factor, where V_f is the flight speed, ω_t the turn rate and γ the flight path angle. The corresponding bank angle ϕ_t is then given by

$$\cos\phi_t = \frac{1}{n_t} \tag{3}$$

where ϕ_t is the lateral tilt of the vector of magnitude n_t away from the vertical. For the simulation results discussed in this Paper, the difference between the helicopter roll attitude ϕ, and ϕ_t is so small that they can be considered interchangeable when interpreting curves that are functions of ϕ.

2.2 Variations in flight dynamics with bank angle

The detailed analysis in this paper is made for right turns of bank angles up to 60° and at airspeeds of 60 and 100 kn. Reference will also be made to equivalent left turns and 80 kn speed where appropriate. The helicopter was modelled in its linearised six-degree-of-freedom form as an Aerospatiale SA330 Puma, Fig 1, using the mathematical model HELISTAB[5].

2.2.1 The stability and control derivatives

The stability and control derivatives are plotted as a function of body roll attitude ϕ (Phie) in Fig 2 for left and right turns up to 2 g at 60, 80 and 100 kn. Derivatives are normalised by mass and moments of inertia where appropriate *ie* Z_w has units of s^{-1} and L_v has units $(ft.s)^{-1}$. The causes of the variations with bank angle (aerodynamic, inertial, gravitational and kinematic) have already been discussed by Chen *et al*[1] - Fig 2 is intended to be used as a reference, as it describes the changes to the helicopter's equations of motion over quite a large part of the flight envelope. Nonetheless it is fruitful to briefly discuss overall trends and to highlight the implications of some of the changes in individual derivatives. The effect of bank angle (or, more correctly, rotor thrust and turn rate) is seen to be marked for a large number of the derivatives, with increases in magnitude being a common feature. Considering in more detail derivatives that might have influence on the short term longitudinal motion, the conventional aeroplane short period approximation, applied to the helicopter and including longitudinal cyclic control terms, can be written,

$$\begin{bmatrix} \dot{w} \\ \dot{q} \end{bmatrix} = \begin{bmatrix} Z_w & Z_q \\ M_w & M_q \end{bmatrix} \begin{bmatrix} w \\ q \end{bmatrix} + \begin{bmatrix} Z_{\theta_{1s}} \\ M_{\theta_{1s}} \end{bmatrix} \theta_{1s} \qquad (4)$$

With reference to Fig 2, it can be seen that (4) will predict an increase in pitch rate response sensitivity and a generally faster primary rate response as bank angle is increased though the increases in damping (M_q) and control power ($M_{\theta_{1s}}$). Further, these variations in the primary response will be the same in left and right turns. Turning to the cross coupled responses, N_w and N_q numerically increase in a 2 g turn to either the left or right as does L_w, and to a lesser extent in left turns only, L_q. Use of longitudinal cyclic pitch for primary axis control therefore is likely to excite yawing and rolling motion - especially as sideslip and yaw damping, as indicated by Y_v and N_r do not increase to nearly the same extent. These cross couplings will additionally affect the primary axis response, as evinced by the considerable increase in M_v (due principally to the increase in rotor thrust and coning) in both left and right turns, and that in M_p, although in the latter case this is so only in left turns.

2.2.2 Variation in the response modes with bank angle

The variation in all the rigid body response modes with bank angle in turns up to 2 g at 100 kn is shown in Fig 3. This figure contains turns to the left to show the non-symmetrical changes in the modes with bank angle. Fig 3a illustrates more clearly by isolation the longitudinal short period complex conjugate pair of eigenvalues, in level flight and right turns, which represents the mode of concern to the present study. Note that the mode damping and frequency do not change significantly with bank angle: the important changes though are in the character of this mode, Table 1.

The mode retains its longitudinal character, although cross coupling with roll rate and to a greater extent sideslip, increases with increasing bank angle.

The situation at 60 kn is rather different, Fig 4. In this figure the longitudinal short period mode cannot be presented in isolation for the full range of bank angles studied, due to the fact that it coalesces with two others. The additional (initially non-oscillatory) eigenvalues plotted belong to the lateral-directional set: the large modulus mode on the left is the "roll" mode, that on the right the "spiral" mode. With increasing bank angle the damping of the short period longitudinal mode remains approximately constant, but the frequency is reduced until at about $\phi_t = 50°$ this pair of eigenvalues meet the real axis and split to form a pair of pure subsidences. One moves to the left, meeting and coalescing with the roll mode to form a complex conjugate pair the damping of which remains roughly constant with further increase in bank angle, but the frequency increases; the other mode moves to the right and forms a complex conjugate pair of eigenvalues with the spiral mode in a similar fashion.

Table 2 contains the eigenvectors of the short period longitudinal mode at this speed (except for the 60° bank angle, where the eigenvector is that of the large modulus complex pair, the formation of which has just been described). Like the 100 kn cases, there is increased cross coupling with sideslip and roll rate with increasing bank angle. Additionally, there is increased cross coupling with speed, which itself grows with increasing bank angle. These differences in the 60 kn results are intriguing - especially the effect of bank angle on the eigenvalues between angles of 45° and 60° - and will be addressed in a later section.

2.2.3 Variation in the time responses with bank angle

The response of the helicopter model to a doublet input (at 0.5s) in longitudinal cyclic pitch of magnitude 1° and period 4.5 s is shown in Figs 5 and 6. This doublet was chosen as its peak spectral power level occurs approximately at the resonant frequency of the short period mode at 100 kn. The primary responses w and q are given, together with those in v and p, since the eigenvectors of the short period longitudinal mode indicate that cross coupling increases significantly into these modes.

The primary axis responses at 60 and 100 kn demonstrate increasing control sensitivity with bank angle, no overshoot tendency in the short term, and roughly similar damping. The cross coupled responses too, increase with bank angle. This is particularly true at 100 kn, where the magnitude of the cross coupled responses relative to the primary axis response indicates strong cross coupling in the short term at high bank angle. At 60 kn, although the cross coupled responses increase with bank angle, their magnitude relative to the primary response in the short term is not nearly as great as at 100 kn, especially in sideslip.

It is worthwhile to remember at this stage that the responses presented in Figs 5 and 6 do not necessarily show purely the short period longitudinal mode being excited - the overall response is a

sum of the responses of individual modes to the input. There could be a considerable contribution to the overall response for example from dutch roll, which has a frequency close to that of the short period longitudinal mode. This point is considered further in a later section.

3 SIMPLE REDUCED-ORDER MODELS

3.1 Modal characteristics

It would seem that the changes with bank angle to the longitudinal short period mode described in section 2.2.2 are due to increased cross coupling derivatives. Some idea of the impact of these derivatives on the mode eigenvalues in turns is provided by comparing the eigenvalues of the full system with those of the reduced order model formed by the usual approximation for the conventional aeroplane short period mode, given by the autonomous form of (4), viz,

$$\begin{bmatrix} \dot{w} \\ \dot{q} \end{bmatrix} = \begin{bmatrix} Z_w & Z_q \\ M_w & M_q \end{bmatrix} \begin{bmatrix} w \\ q \end{bmatrix} \tag{5}$$

Fig 7, for the 60 kn turns, indicates that the structure represented by (5) adequately predicts mode frequency and damping up to bank angles of about 45°. The significant discrepancy at the 60° bank angle is due to the effect described in section 2.2.2, and not to a severe change in the trend that the diagram might at first suggest. Fig 8, for the 100 kn turns, shows a more gradual breakdown in the approximation to the mode frequency, and up to bank angles of 45°, a constant error of about 10% in mode damping. In terms of magnitude, the approximation is in error by about 15% at 60° bank angle.

Another possible reduced order model structure[6], includes the roll degree of freedom and the associated cross coupling derivatives, viz

$$\begin{bmatrix} \dot{w} \\ \dot{q} \\ \dot{p} \end{bmatrix} = \begin{bmatrix} Z_w & Z_q & Z_p \\ M_w & M_q & M_p \\ L_w & L_q & L_p \end{bmatrix} \begin{bmatrix} w \\ q \\ p \end{bmatrix} \tag{6}$$

In view of the fact that the eigenvectors of the short period longitudinal mode contain roll rate, which increases in magnitude with bank angle, (6) appears to be more applicable to the manoeuvring flight cases than (5). However, the stability diagrams for 60 and 100 kn, Figs 9 and 10 respectively, indicate that the situation is yet more complex than that described by (6). At 100 kn, the agreement improves up to bank angles of 30°, and thereafter worsens considerably - mode damping is overestimated by 50%, while the error in frequency is similar to that given by (5). At the 60 kn speed the approximation still appears invalid at high bank angle although an improvement on the behaviour by (5). Nevertheless, it does not, on further examination, predict the trend with bank angle accurately - the location represented at the 60° point on Fig 9 has

not been reached in the same manner as that of the full system, by meeting the real axis, splitting and forming two complex conjugate pairs. Rather, the approximation gives a steady reduction in mode frequency, from the accurate approximation in level flight, to the value in Fig 9.

3.2 Time response characteristics

The response of the approximation (4) to the same input as that used in section 2.2.3 is given for the three bank angles 0°, 45° and 60°, in Fig 11 for 60 kn, and Fig 12 for 100 kn. Although differences are discernable between full and approximate system responses at the various speed and bank angle combinations, the approximation really is very good at predicting the short term pitch rate response to the input in longitudinal cyclic. Therefore the approximation is useful for predicting features of the short term rate response that affect handling qualities, highlighted in Ref 7, such as control sensitivity, delay time, time constant and the steady state following the input. Prediction of w though, worsens with increasing bank angle, more so at 60 than 100 kn. This implies that the prediction of normal acceleration in the short term, particularly its peak value, will be in error. Normal acceleration response is not only an important cue for the pilot, but also can be used as a measure of handling qualities - the original critera[8] for longitudinal control response, the NACA divergence requirement, was expressed in terms of features of the normal acceleration response. As can be seen from Fig 13, at 60° bank angle and 100 kn, the normal acceleration response predicted by (4) is in error; not just the peak value - there are differences in the shape of the two responses in the short term, and, as pointed out in Ref 8, the shape of the response is as important as the peak value.

Fig 14 compares the response of the approximation (6), plus appropriate control terms, with the full system at the 100 kn, 60° bank angle condition. The primary axis response shows similar comparison with the full system to that of the approximation (4). The cross coupled response however is wrongly predicted, both in magnitude and sign, over the time interval.

3.3 Use of the approximations and the nature of the response

The real value in using reduced order models is that high order systems can be viewed as the sum of conceptually simpler subsystems, thus allowing clearer insight into the nature of various modes, ie what terms are adequate for describing the dynamic characteristics of interest. Additionally, one can then use these sub-models in parametric studies, examining the effects on the dynamics by varying the elements of the subsystem. The approximations that have just been examined seem adequate for representing short term pitch rate response, and therefore appear to be useful for assessing aspects of the primary axis response that impact longitudinal handling qualities. However, the normal acceleration response is in error, and the approximation does not predict the very substantial cross coupled responses that are generated in the short term in the high bank angle turns, especially at 100 kn. The inclusion of these effects in studies of short period longitudinal motion could be required if they are sufficient to degrade the short term longitudinal handling qualities, or to mask basically good qualities because

excessive pilot workload is required for compensation. Furthermore, the approximations are inadequate for representing the short period mode eigenvalue in the high bank angle turns. In addition to the inadequacies of the approximations, there appears to be a contradiction in the results, highlighted by the pitch rate response comparisons, *ie* the approximations predict primary axis dynamic characteristics (the mode eigenvalues) that are considerably in error at the high bank angles, yet the primary axis time response of the approximations compares well with those of the full system in the short term. This tends to indicate that the short term longitudinal motion is made up, not just of the short period mode excitation, but also of other modes that contain pitch rate motion.

These results therefore suggest that the cross coupling terms need to be included in a modified approximation in order that the nature of the primary axis response is correctly represented. The approximation would then be more applicable for parametric studies, as well as giving insight into the nature of the short term longitudinal dynamics. The results can also be confirmed from an order of magnitude analysis of the coupling effects. In general, conditions for 'weak coupling'[9] and hence, valid subsystem decomposition, are met if, in a dynamic system partitioned into a series of interconnected subsystems, the subsystem eigenvalues are well separated in modulus and the coupling terms are, in a relative sense, small. However, it can be shown that both of these conditions are violated in turning flight at high bank angles for the examples shown in this Paper.

4 AN ANALYTICAL TECHNIQUE

In view of these results, which indicate strong rather than weak coupling, a methodology used previously[10] has been further developed and applied to the helicopter in manoeuvring flight. The system matrix is partitioned into two subsystems, one of which is to represent the mode of concern, and a transformation is applied to the system of equations. The result is a matrix identity made up of the mode eigenvalues and terms involving the submatrices of the full system. The numerical importance of terms satisfying the identity is used to highlight the significance of individual derivatives to the mode. The technique is also used as a rational approach for identifying lower order model structures that will approximate modes of interest.

The state-space description of the helicopter,

$$\dot{\underline{x}} = A\underline{x} + B\underline{u} \tag{7}$$

is transformed into a new set of state variables using the canonical transformation,

$$\underline{x} = E\underline{z} \tag{8}$$

E is the matrix of eigenvectors of A such that E(j,i) is the jth element of the ith vector of A associated with the eigenvalue λ_i . z is the n-dimensional transformed state vector. Thus (7) becomes

$$\dot{\underline{z}} = \Lambda \underline{z} + R\underline{u} \;,\; R = E^{-1} B \tag{9}$$

Now from (9) and (7), writing $F = E^{-1}$,

$$\Lambda = FAE \tag{10}$$

and it can be shown that $\Lambda = \text{diag}\,[\lambda_i]$, $i = 1, n$ by considering the defining condition on the eigenvectors

$$(\lambda_i I - A)\,\underline{e}_i = 0 \tag{11}$$

These are established results and can be found in most texts dealing with linear systems analysis. However, through manipulation of (10) and consideration of the numerical significance of terms contained in the resulting identities, a methodology can be developed to provide a rational means of identifying important coupling derivatives. The state vector is now assumed to be ordered

$$\underline{x} = [\, w\ q\ u\ \Theta\ v\ p\ \phi\ r\ ]^T$$

and the system matrix A partitioned such that,

$$A = \begin{bmatrix} A_{11} & A_{12} \\ A_{21} & A_{22} \end{bmatrix} \tag{12}$$

A_{11} is a 2 x 2 matrix that contains the structure of the traditional short period approximation (4), viz

$$A_{11} = \begin{bmatrix} Z_w & Z_q \\ M_w & M_q \end{bmatrix} \tag{13}$$

A_{12} and A_{21} are the coupling matrices and A_{11} (and therefore the w and q motions) will be decoupled from the rest of the system if either one is null, or in a relative sense close to null. The approximation (4) will then be a valid one. It has been shown that this is not the case for high bank angle turning flight and the aim in developing the methodology is to evaluate the nature of the coupling.

If (10) is partitioned such that it contains A in the partitioned form found in (12), then

$$\begin{bmatrix} \Lambda_1 & 0 \\ 0 & \Lambda_2 \end{bmatrix} = \begin{bmatrix} F_{11} & F_{12} \\ F_{21} & F_{22} \end{bmatrix} \begin{bmatrix} A_{11} & A_{12} \\ A_{21} & A_{22} \end{bmatrix} \begin{bmatrix} E_{11} & E_{12} \\ E_{21} & E_{22} \end{bmatrix} \tag{14}$$

The diagonal matrix Λ_1, in this case, contains the short period longitudinal eigenvalues. By performing a simple matrix algebra operation the matrix identity for the eigenvalues Λ_1 is obtained

$$\Lambda_1 = F_{11}A_{11}E_{11} + F_{11}A_{12}E_{21} + F_{12}(A_{21}E_{11} + A_{22}E_{21}) \tag{15}$$

The identity is a sum of n^2 terms, each one of which contains a derivative factored by the relevant elements of the F and E matrices. The importance of each of the n^2 terms to satisfying the identity is used as a measure of the significance of the relevant derivative to the mode.

The identity (15) can be used in a formal approach to the synthesis of a rational approximation to the mode. Consider the autonomous form of (7) partitioned as in (12). Then

$$\dot{\underline{x}}_1 = A_{11}\underline{x}_1 + A_{12}\underline{x}_2$$

$$\dot{\underline{x}}_2 = A_{21}\underline{x}_1 + A_{22}\underline{x}_2$$

where $\underline{x}_1 = [w\ q]^T$, and A_{11} is given by (13). Then the eigenvalues of interest are given by,

$$\det\left[\lambda I - A_{11} - A_{12}(\lambda I - A_{22})^{-1} A_{21}\right] = 0$$

Now as $A_{12} \to [0]$ (or $A_{21} \to [0]$) then

$$\det\left[\lambda I - A_{11}\right] \to 0$$

and consideration of the defining conditions on the eigenvectors, (11), shows that

$$E \to \begin{bmatrix} E_{11} & 0 \\ 0 & 0 \end{bmatrix}$$

ie, the dynamics represented by A_{11} (and thus w and q) become decoupled from the rest of the system. Inspection of (15) shows that under the same conditions

$$F_{11}A_{11}E_{11} \to \Lambda_1 \tag{16}$$

$$F_{11}A_{12}E_{21} + F_{12}(A_{21}E_{11} + A_{22}E_{21}) \to [0] \tag{17}$$

The terms on the left hand side of (17) can thus be considered as coupling terms and a quantifiable measure of the coupling. If the structure represented by A_{11} does not give an adequate approximation to the mode, the derivatives in the significant terms on the left hand side of (17) can indicate whether a re-partitioning is possible for (16) and (17) to be fulfilled.

5 RESULTS

5.1 The 100 kn flight condition

The terms in the identity (15) for the short period longitudinal eigenvalues are shown in Table 3a for the range of bank angles 0, 15, 30, 45 and 60° at a flight speed of 100 kn. As bank angle increases, the importance of coupling terms increases. Table 3b gives a breakdown of the coupling contributions, for the terms in

$F_{11}A_{12}E_{21}$, as a sum of the products of each derivative in A_{12} with the relevant eigenvector terms. The pitching moment cross coupling M_p dominates the part of the identity involving A_{12} in level flight and at small bank angles (up to 30°). The contribution from M_v however, already increasing with bank angle, becomes significant at and above bank angles of 45° to the extent that for a turn with 60° of bank, the importance of the M_v term to the identity is as significant as that of M_p . Two other numerically important terms in $F_{11}A_{12}E_{21}$ (although smaller than those involving M_p or M_v) are those associated with Z_ϕ and, to a lesser extent, M_u .

The derivatives are made up of contributions from several sources, *eg* fuselage, rotor, gravitational, inertial. The variation of M_v , M_p and Z_ϕ , together with their components, is given in Fig 15. M_v is purely a rotor effect due to increased thrust and coning as currently modelled, and increases with bank angle. M_p has rotor and inertial terms and, overall, also increases with bank angle. The effect of the inertial contribution to M_p in a left turn can be found from Fig 2 - the asymmetry in the shape of the M_p curves arising from the fact that in the corresponding left turn, the inertial term has the same magnitude, but opposite sign, while the variation in the rotor contribution is almost the same for both left and right turns. The derivative Z_ϕ is made up entirely of a gravitational term. The sources of these changes to the derivatives M_v , M_p and Z_ϕ can be found from the equations of motion of the aircraft, viz,

$$I_{yy}\,\dot{q} = (I_{zz} - I_{xx})rp + I_{xz}\,(r^2 - p^2) + M \qquad (18)$$

$$\dot{w} = -(vp - uq) + \frac{Z}{m} + g\cos\theta\cos\phi \qquad (19)$$

and the approximate expression for the pitching moment, M_R , due to rotor thrust, T , is given by,

$$M_R = -Tx_{cg} - T\,(\gamma_s + \beta_{1c})h_R \qquad (20)$$

Here $\dot{q}$ is the pitch acceleration, M the applied pitching moment, I_{xx} , I_{yy} , I_{zz} the roll, pitch and yaw moments of inertia, and I_{xz} the roll/yaw product of inertia. Z is the applied heave force and m the aircraft mass. β_{1c} is the longitudinal disc flapping, γ_s the shaft tilt and x_{cg} and h_R the cg position ahead of and below the rotor hub.

Then $\partial M/\partial\alpha$, α being any state variable, is given by,

$$\partial M/\partial\alpha = -\partial T/\partial\alpha\,(x_{cg} + (\gamma_s + \beta_{1c})h_R) - Th_R\,\partial\beta_{1c}/\partial\alpha \qquad (21)$$

From (18), it can be seen that there will be an inertial contribution to the M_p derivative. From (19), the gravitational Z_ϕ can be identified. Finally, the most obvious change to the derivative $\partial M/\partial \alpha$ in turning flight is due to the increased rotor thrust. At the 60° bank angle flight condition, for example, the thrust has doubled compared with its 1 g level flight value.

5.2 The 60 kn flight condition

The 60 kn case is especially interesting because of the change in character of the short period mode with increasing bank angle, as illustrated in section 2.2.2. The identities for 60 kn are presented in Table 4a and the constituents of the term $F_{11}A_{12}E_{21}$ in Table 4b. As with the results for 100 kn, M_v and M_p are the major cross coupling derivatives. However M_u has assumed an increased significance at the high bank angle. A breakdown of the derivatives gives the same result as for 100 kn - the increasing rotor contribution to M_u, M_v and M_p dominate the change with bank angle.

5.3 Improved model structures

Synthesis of rational approximations to the short period longitudinal mode not only helps to validate the methodology described in section 3, but goes some way to highlighting the nature of the helicopter's short term motion in high bank angle turns. The following analysis is carried out only for the 60° bank angle turns, at 60 and 100 kn.

As was seen in section 4.1 the strongest cross coupling derivatives were M_v and M_p at 100 kn. Re-ordering the state vector $\underline{x}$, and partitioning the system matrix so that M_v and M_p are included in A_{11}, gives the following result:

Full system eigenvalue $-1.0540 \pm 1.4380i$
Approximate eigenvalue $-1.0506 \pm 1.3093i$

The new structure also includes yaw rate terms so that the dutch roll mode is adequately represented, *ie*,

$$A_{11} = \begin{bmatrix} Z_w & Z_q & Z_p & Z_v & Z_r \\ M_w & M_q & M_p & M_v & M_r \\ L_w & L_q & L_p & L_v & L_r \\ Y_w & Y_q & Y_p & Y_v & Y_r \\ N_w & N_q & N_p & N_v & N_r \end{bmatrix} \qquad (22)$$

The imaginary part of the eigenvalue is still in error, by about 9%. The other terms in the matrix A_{12} that the identity suggests are important are Z_ϕ, followed by M_u. Now, including only the strongest three cross coupling terms M_v, M_p and Z_ϕ in the approximation,

$$A_{11} = \begin{bmatrix} Z_w & Z_q & 0 & 0 & Z_\phi & 0 \\ M_w & M_q & M_v & M_p & 0 & 0 \\ Y_w & Y_q & Y_v & Y_p & Y_\phi & Y_r \\ L_w & L_q & L_v & L_p & 0 & L_r \\ N_w & N_q & N_v & N_p & 0 & N_r \\ 0 & 0 & 0 & 1 & 0 & 0 \end{bmatrix} \quad (23)$$

gives the following result,

Full system eigenvalue $-1.0540 \pm 1.4380i$
Approximate eigenvalue $-1.1300 \pm 1.4623i$

The approximation to the frequency is now very good while the damping is in error by about 6%. Including M_u in (25) will improve this considerably. The nature of the cross coupling suggested by the significant terms in the identity, is confirmed by the differing validity of the various approximations (4), (6), (22) and (23). The response of the approximation (23), plus appropriate control terms, to the doublet input, is shown in Fig 16. Improved comparisons of both primary axis and coupled responses are evident over the time interval. Beyond about 3s, other modes begin to contribute to the response. Nonetheless, in the important short term, primary and coupled responses are well predicted, in both magnitude and shape.

The major difference in the results for 60 kn is the much larger contribution to the identity of the term involving M_u. A satisfactory approximation can then only be devised by including the speed effects (M_u) in the model structure, whence the dimension of the approximate subsystem has nearly returned to the full system.

6 ANALYSIS OF FLIGHT TEST RESULTS

Flight test data obtained during trials using the RAE Bedford Puma flight research helicopter were analysed to determine whether the short term longitudinal motion was cross coupled with sideslip, and what the pilot's compensatory control activity (if any) would be in such circumstances. This coupling was chosen because of its significance to the short period mode as predicted by the results in the preceding sections, and the fact that it would require the use of an extra control, the pedals, for compensation. Data from a low level circle-following flying task, was analysed. The task was flown at a nominal 90 kn and load factor of 1.8. For the purposes of a study such as this, the use of data from an applied flying task can make analysis difficult because the pilot control strategy is determined, not just by natural aircraft handling characterisitics, but by external influences. These include wind effects, task cues and the level of workload used, and hence performance achieved.

Power spectra of the pilot's longitudinal cyclic stick (η_{ls}) and pedal (η_p) activity are shown in Fig 17, illustrating one external influence that is strong enough to dominate the pilot's control strategy at low frequency, that is, the effect of wind, dominating

the control activity below 0.1 Hz. At the higher frequencies there are peaks in cyclic control activity at 0.25, 0.35 and 0.43 Hz, and in pedal activity at 0.10 and 0.25 Hz. Only at 0.25 Hz therefore are pedal and cyclic used together. Coherency and cross amplitude spectra for the input-output pairs (w,η_{1s}) and (q,η_{1s}) are given in Fig 18. Coherency levels of between 0.8 and 0.9 result at frequencies of about 0.25 Hz, and 0.7 to 0.8 between 0.35 and 0.43 Hz, for (w,η_{1s}). Coherency levels at these frequencies for(q,η_{1s}) are between 0.9 and 1. This tends to indicate near-linearity in the relationships between these longitudinal variables and η_{1s}. Apart from low frequency activity to compensate for the effects of wind, the level of cross spectral power tends to indicate that longitudinal control is predominantly at 0.25 Hz, and to a slightly lesser extent at 0.35 Hz. Now the cross amplitude spectra for (v,η_p), Fig 19, show peak power levels (again apart from the low frequency peaks) at 0.25 Hz, but only for (v,η_{1s}) is there a peak at 0.35 Hz. Pedal, which is used mainly for compensation, is correlated with sideslip at 0.25 Hz - where cyclic is being used for longitudinal control. Unfortunately this correlation in frequency between longitudinal response, sideslip response, and the peak in compensatory activity, is not conclusive proof of short period mode pitch-sideslip cross coupling. This is principally because the aircraft response is a sum of the contributions from all the modes that have been excited, *eg* the sideslip response at 0.25 Hz will be the sum of that due to longitudinal short period and dutch roll motion. This will affect any assessment of the pilot's pedal control strategy.

These results do not therefore, provide a conclusive explanation, although the analysis has only been made of the most obvious features of the spectra that are likely to highlight the cross coupled response, and the required control strategy. Data from a range of applied flying tasks together with more clinical manoeuvre stability tests are currently being analysed at RAE. These studies should highlight handling characteristics that increase compensatory pilot control activity, and hence workload, for precise low level flying tasks, and results will be reported at a later date.

7 DISCUSSION

The validity of the conventional fixed wing aeroplane approximation to the short period longitudinal mode of the articulated rotor helicopter in high bank angle turns, has been explored. Results presented for a Puma helicopter in the mid-speed range indicate that the eigenvalues of the approximation are in error and the approximation will not contain the increase in cross coupling that the eigenvectors of the full system predict. Furthermore, the time responses are such that characteristics that are important to the assessment of short term longitudinal handling qualities, such as normal acceleration response, are poorly predicted. In addition, the cross coupled responses, in the short term, are large, and this could affect any assessment of short term longitudinal handling qualities in the real aircraft. Their inclusion in models of short term longitudinal motion could therefore be necessary. The inaccuracy of the conventional approximation arises because of coupling with degrees of freedom that are not represented in the structure of the reduced system, and this coupling is strong rather than weak.

It could however be argued that the approximation is useful in that it predicts trends in the primary axis response with increasing bank angle, as well as trends in mode eigenvalues. Nevertheless, it does not represent the nature of the short term response accurately, because of the strong coupling with other degrees of freedom. Therefore, because parameters that have a strong influence on the short term longitudinal mode are not included in the approximation, its use for parametric studies could lead to errors in the prediction of short term characteristics.

For the cases studied, the analysis has shown that coupling with roll rate, sideslip, bank angle and speed perturbations contribute to the motion, the major effects being due to roll rate and sideslip, through the pitching moment derivatives M_v and M_p. Aerodynamic contributions to these derivatives dominate their increase with bank angle, although the inertial term has some effect on M_p. The coupling with bank angle perturbations is due to the gravitational term in Z_ϕ increasing with bank angle.

The methodology described has proved useful for identifying cross coupling derivatives that are significant in their effect on the short period longitudinal mode, and the omission of which from lower order models invalidates the conventional, as well as other, more complex approximations to this mode in high bank angle turns. The technique has proved useful in highlighting the extent of the strong coupling; it could alternatively be applied to systems where a weaky coupled reduced order model structure is not at first apparent. In such circumstances, the methodology could be viewed as a preceding step to the method of weakly coupled systems, identifying a state vector ordering and system partitioning that defines cross couplings as 'weak'. Construction of approximations to the short term longitudinal mode helps to validate the methodology, and highlights the complex interaction of various parameters that influence the mode; the 60 kn result is an especially complex situation. The value of these approximations however (aside from highlighting the nature of the cross coupling) may be limited by their high order, and it could be that in practical applications, these approximations offer little benefit over the full system description.

8 CONCLUSIONS

Short term longitudinal motion is more complex in nature in high bank angle turns than in level flight. Consequently, for the examples studied it has been shown that the conventional short period mode approximation is inadequate for predicting stability and response characteristics, although it does predict general trends with increases in bank angle. The approximation fails because the cross coupling is strong rather than weak.

All the derivatives change with bank angle, the trend being generally to increase in magnitude with increasing bank angle. The variations in the derivatives are due to aerodynamic, inertial, kinematic and gravitational terms; however it is principally the increased aerodynamic term (due to increased rotor thrust and coning) that affects the short period approximation through the derivatives M_v and M_p. An increased gravitational effect,

through the derivative Z_ϕ also contributes to increased cross coupling, although to a lesser extent than the aerodynamic terms.

Since increasing rotor thrust is a fundamental element of manoeuvring, its effect on cross coupling will tend to be similar in more general manoeuvres. The effect of inertial and gravitational terms is, however, likely to be more manoeuvre-specific, since they depend, for the terms highlighted in this paper, on the kinematics of the manoeuvre. It is emphasised that the results described do not necessarily indicate general trends for all helicopters and some are likely to be configuration specific. Nevertheless, the scope of the increased complexity has been illustrated and future effort will be directed towards the derivation of more general results.

The methodology adopted to analyse the response modes offers a useful means of quantifying cross coupling, highlighting important derivatives and indicating forms of approximation for aircraft modes.

Flight data were analysed to determine whether sideslip coupling in short term longitudinal motion is noticeable in practice and the extent of compensatory activity required to maintain accurate flight path control at low level. Results of this analysis are, however, inconclusive, although the complex nature of the applied flying task is almost certainly a contributory factor here.

REFERENCES

1) R.T.N. Chen, Flight dynamics of rotorcraft in steep high-g turns. Paper presented at the AIAA 9th Atmospheric Flight Mechanics Conference, (1982).

2) R.T.N. Chen, J.A. Jeske, R.H. Steinberger, Influence of sideslip on the flight dynamics of rotorcraft in steep turns at low speeds. Paper presented at the 39th Annual National Forum of the American Helicopter Society, (1983).

3) R.B. Lewis II, Hueycobra manoeuvring investigations. Procedings of the 26th Annual National Forum of the American Helicopter Society, (1970).

4) R.T.N. Chen, J.A. Jeske, Influence of sideslip on the kinematics of the helicopter in steady coordinated turns. Paper presented at the 37th Annual Forum of the American Helicopter Society, (1981).

5) J. Smith, An analysis of helicopter flight mechanics: part 1 user's guide to the software package HELISTAB. RAE Technical Memorandum FS(B) 569, (1984).

6) G.D. Padfield, On the use of approximate models in helicopter flight mechanics. Vertica Vol. 5, (1981).

7) G.D. Padfield, Flight testing for performance and flying qualities. AGARD LS 139, (1985).

8) F.B. Gustafson, *et al* , Longitudinal flying qualities of several single-rotor helicopters in forward flight. NACA TN 1983, (1949).

9) R.D. Milne, The analysis of weakly coupled dynamical systems. Int. J. Control 2, No. 2, (1965).

10) S.S. Houston, On the benefit of an active horizontal tailplane to the control of the single main and tail rotor helicopter. Ph. D. Dissertation, University of Glasgow, (1984).

Table 1

EIGENVECTOR ELEMENTS FOR SHORT PERIOD LONGITUDINAL MODES, 100 KN

Longitudinal states				
ϕ_t	u	w	q	θ
0	0.1183±0.0170i	0.8600i	-0.0010±0.0257i	0.0122±0.0073i
15	0.1192±0.0237i	0.8491i	-0.0006±0.0246i	0.0117±0.0096i
30	0.1209±0.0370i	0.7972i	-0.0006±0.0220i	0.0097±0.0119i
45	-0.0868±0.1055i	-0.1810±0.6659i	-0.0166±0.0054i	0.0124±0.0098i
60	-0.1226±0.0904i	-0.1818±0.4562i	-0.0087±0.0042i	0.0160±0.0083i
Lateral/Directional States				
ϕ_t	v	p	ϕ	r
0	-0.1042±0.4817i	0.0172±0.0351i	0.0113±0.0187i	-0.0156±0.0101i
15	-0.1000±0.5010i	0.0176±0.0356i	0.0107±0.0190i	-0.0165±0.0106i
30	-0.1193±0.5751i	0.0191±0.0372i	0.0101±0.0200i	-0.0197±0.0116i
45	0.7080	-0.0434±0.0102i	0.0183±0.0144i	0.0181±0.0207i
60	0.8552	-0.0469±0.0152i	0.0188±0.0152i	0.0210±0.0241i

Table 2

EIGENVECTOR ELEMENTS FOR SHORT PERIOD LONGITUDINAL MODES, 60 KN

Longitudinal States				
ϕ_t	u	w	q	ϕ
0	0.1919±0.0146i	0.8367	-0.0009±0.0265i	0.0158±0.0130i
15	0.2043±0.0365i	0.8329	0.0 ±0.0251i	0.0135±0.0151i
30	0.2237±0.0709i	0.7831	0.0003±0.0213i	0.0083±0.0165i
45	0.2791±0.0193i	-0.5650±0.2824i	-0.0061±0.0113i	0.0103±0.0139i
60	-0.2843±0.0284i	-0.5636±0.0315i	0.0163±0.0010i	0.0079±0.0022i
Lateral/Directional States				
ϕ_t	v	p	ϕ	r
0	-0.4393±0.2580i	0.0107±0.0327i	0.0135±0.0229i	-0.0156±0.0007i
15	-0.4288±0.2760i	0.0110±0.0333i	0.0123±0.0229i	-0.0172±0.0012i
30	-0.4819±0.3106i	0.0106±0.0324i	0.0105±0.0219i	-0.0210±0.0i
45	0.7215	-0.0202±0.0173i	0.0026±0.0180i	0.0206±0.0149i
60	0.7713	0.0398±0.0230i	-0.0234±0.0079i	0.0414±0.0031i

Table 3a

IDENTITIES FOR SHORT PERIOD LONGITUDINAL MODE 100 KN

Real part in					
ϕ_t	A_{11}	A_{12}	A_{21}	A_{22}	Eigenvalue
0	-0.8286	-0.0970	-0.0970	+0.0541 =	-0.9684
15	-0.8263	-0.1010	-0.1010	+0.0492 =	-0.9792
30	-0.8568	-0.1116	-0.1116	+0.0737 =	-1.0063
45	-0.9581	-0.1313	-0.1313	+0.1713 =	-1.0494
60	-1.2599	-0.1615	-0.1615	+0.5289 =	-1.0540
Imaginary part in					
ϕ_t	A_{11}	A_{12}	A_{21}	A_{22}	Eigenvalue
0	+1.4402	+0.0636	+0.0636	-0.0223 =	+1.5450
15	+1.3774	+0.0853	+0.0853	+0.0096 =	+1.5577
30	+1.2686	+0.1175	+0.1175	+0.0503 =	+1.5538
45	+1.0890	+0.1652	+0.1652	+0.1073 =	+1.5267
60	+0.5841	+0.2480	+0.2480	+0.3579 =	+1.4380

Table 3b

COUPLING CONTRIBUTION FOR $F_{11}\ A_{12}\ E_{21}$ - 100 KN

	u		θ		v		p		ϕ		r	
	Re	Im	Re	Im	Re	Im	Re	Im	Re	Im	Re	Im
Z	-0.0037	-0.0006	0.0035	-0.0020	-0.0015	-0.0079	0.0077	0.0169	-0.0018	0.0028	0.0000	0.0000
M	0.0009	-0.0146	0.0000	0.0000	0.0297	-0.0089	-0.1319	0.0780	0.0000	0.0000	0.0000	0.0000
ϕ_t = 0°												
	u		θ		v		p		ϕ		r	
	Re	Im	Re	Im	Re	Im	Re	Im	Re	Im	Re	Im
Z	0.0153	0.0207	0.0014	-0.0026	-0.0001	-0.0387	0.0075	0.0454	-0.1428	0.1764	0.0000	0.0000
M	0.0960	-0.0699	0.0000	0.0000	0.4261	0.0028	-0.5389	0.0844	0.0000	0.0000	-0.0261	0.0296
ϕ_t = 60°												

Table 4a

IDENTITIES FOR SHORT PERIOD LONGITUDINAL MODE, 60 KN

Real part in					
ϕ_t	A_{11}	A_{12}	A_{21}	A_{22}	Eigenvalue
0	-0.7147	-0.1410	-0.1410	+0.1518 =	-0.8448
15	-0.7292	-0.1347	-0.1347	+0.1512 =	-0.8474
30	-0.8195	-0.1301	-0.1301	+0.2273 =	-0.8525
45	-1.2526	-0-0393	-0.0393	+0.5234 =	-0.8077
60	-0.0974	-0.1903	-0.1903	-1.4672 =	-1.9451
Imaginary part in					
ϕ_t	A_{11}	A_{12}	A_{21}	A_{22}	Eigenvalue
0	+1.1863	+0.0047	+0.0047	-0.2074 =	+0.9884
15	+1.1585	+0.0300	+0.0300	-0.2116 =	+1.0067
30	+1.1758	+0.0344	+0.0344	-0.2567 =	+0.9878
45	+1.6416	-0.1311	-0.1311	-0.5434 =	+0.8360
60	+1.0644	+1.6175	+1.6175	-4.0231 =	+0.2763

Table 4b

COUPLING CONTRIBUTION FOR $F_{11}\ A_{12}\ E_{21}$ - 60 KN

	u Re	u Im	θ Re	θ Im	v Re	v Im	p Re	p Im	φ Re	φ Im	r Re	r Im
Z	-0.0133	-0.0003	0.0028	-0.0026	-0.0069	-0.0036	0.0038	0.0100	-0.0020	0.0039	0.0000	0.0000
M	-0.0016	-0.0212	0.0000	0.0000	0.0220	-0.0551	-0.1458	0.0738	0.0000	0.0000	0.0000	0.0000
ϕ_t = 0°												
	u Re	u Im	θ Re	θ Im	v Re	v Im	p Re	p Im	φ Re	φ Im	r Re	r Im
Z	0.0123	-0.0588	-0.0003	0.0008	-0.0014	0.0134	0.0075	0.0168	0.0376	0.1695	0.0000	0.0000
M	-0.1246	0.2552	0.0000	0.0000	-0.2599	0.7020	0.1072	0.6280	0.0000	0.0000	0.0314	-0.1095
ϕ_t = 60°												

Fig 1 RAE Bedford Puma research helicopter

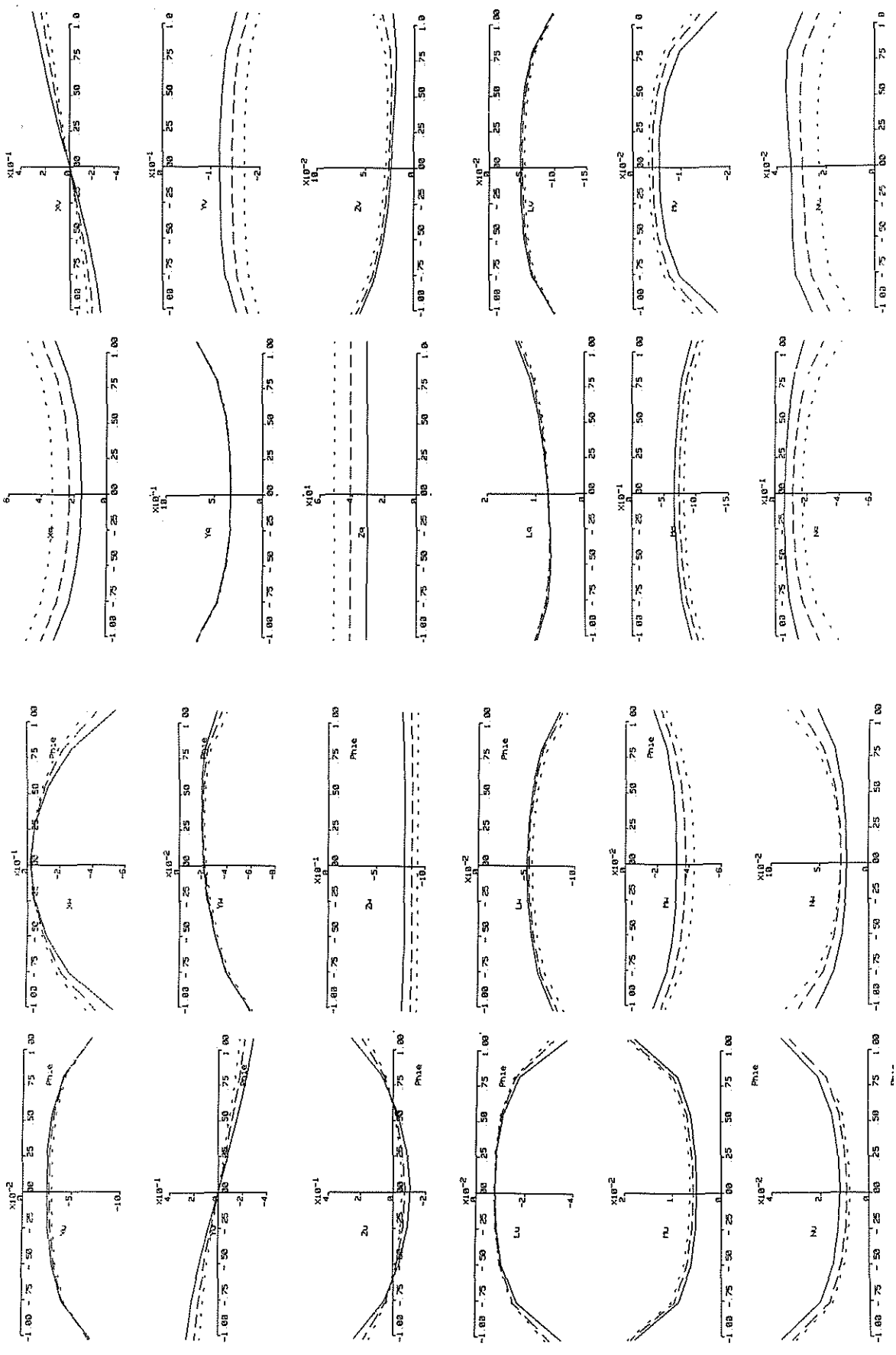

Fig 2 Stability and control derivatives (—— 60 kn,-—80 kn,----100 kn)

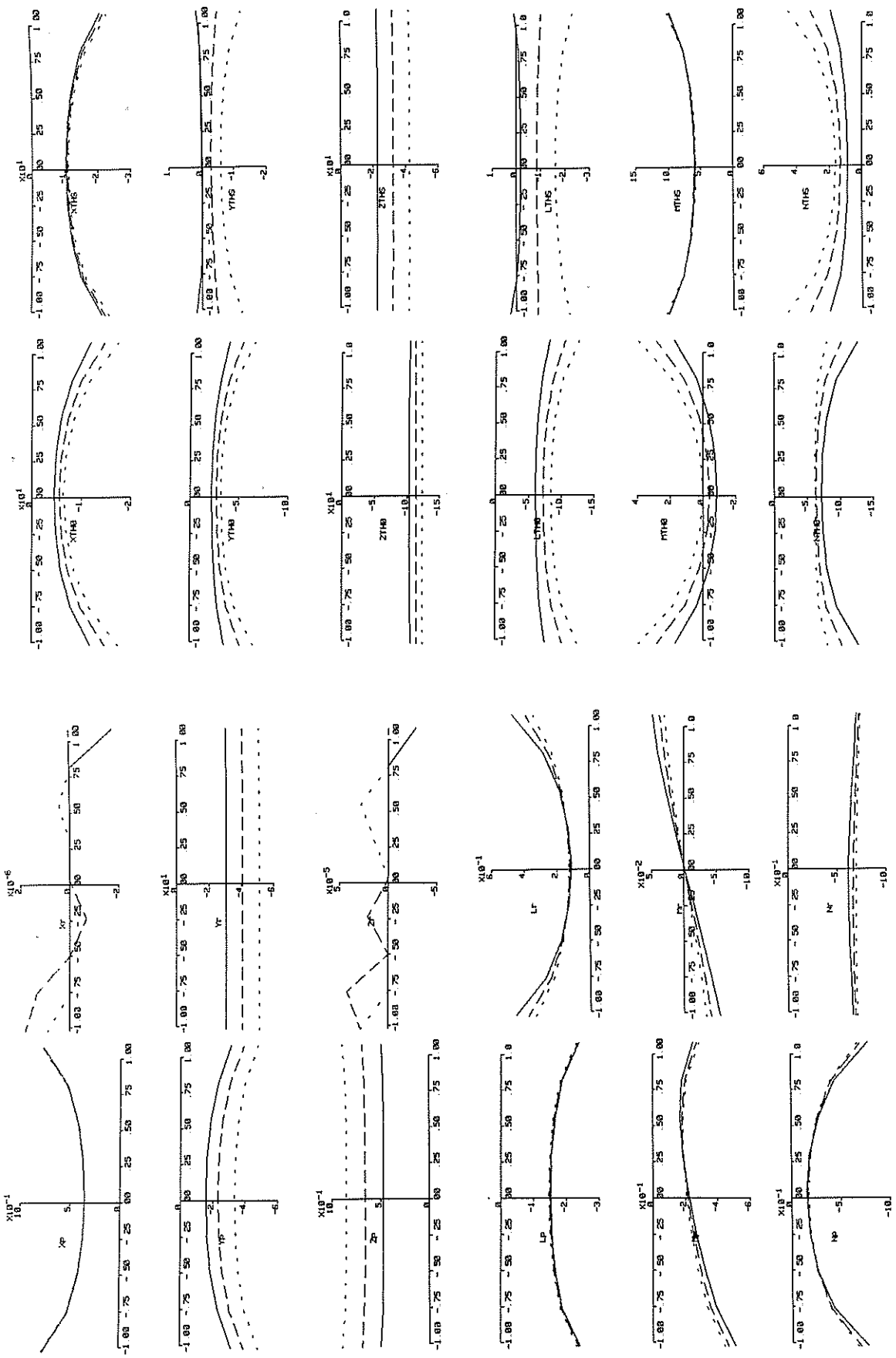

Fig 2 (Continued) Stability and control derivatives
(——60 kn,— — 80 kn,·····100 kn)

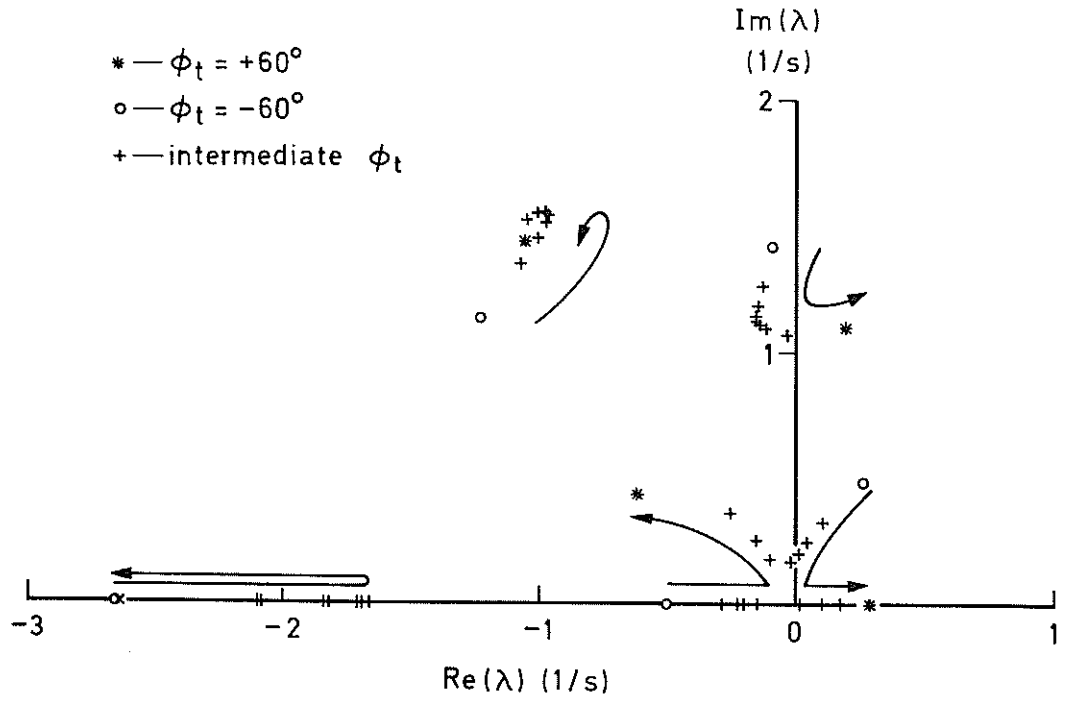

Fig 3 Puma root locus for level turns, 100 kn

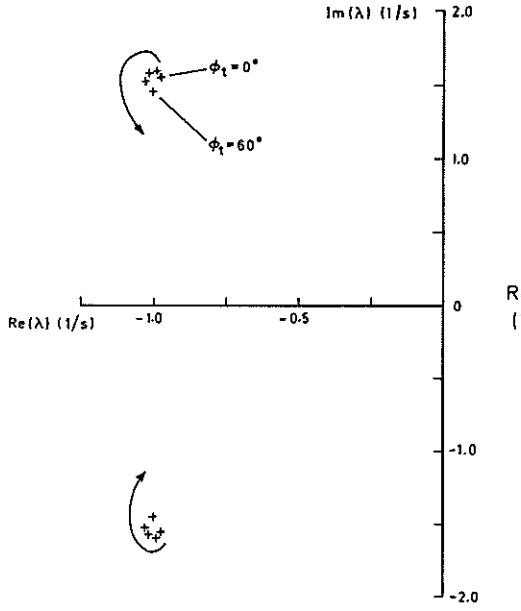

Fig 3a Short period mode root locus, 100 kn

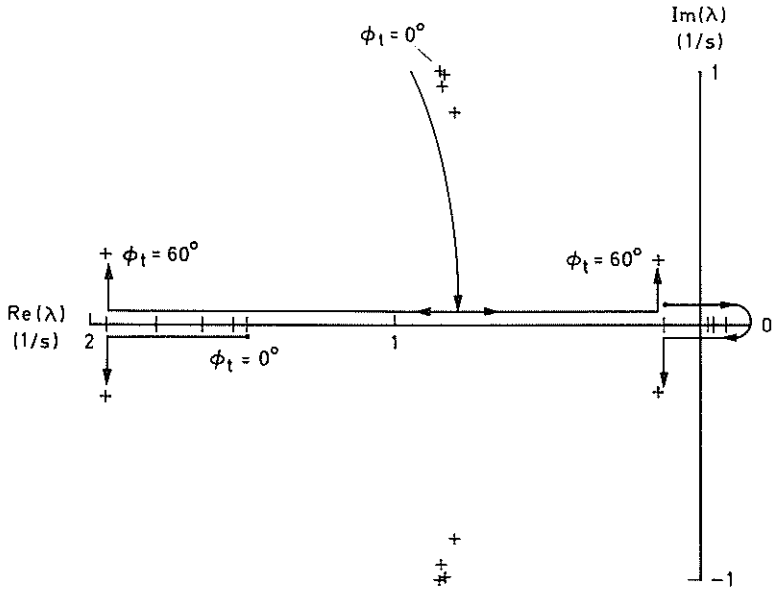

Fig 4 Short period, roll and spiral mode root locus, 60 kn

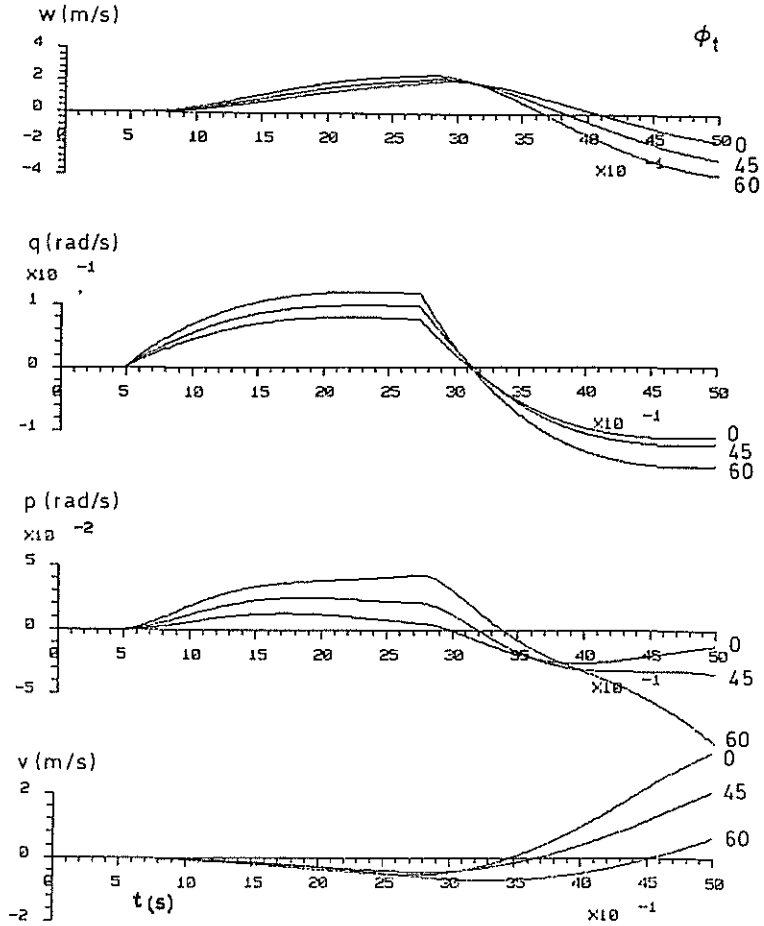

Fig 5 Short term response to longitudinal cyclic input, 60 kn

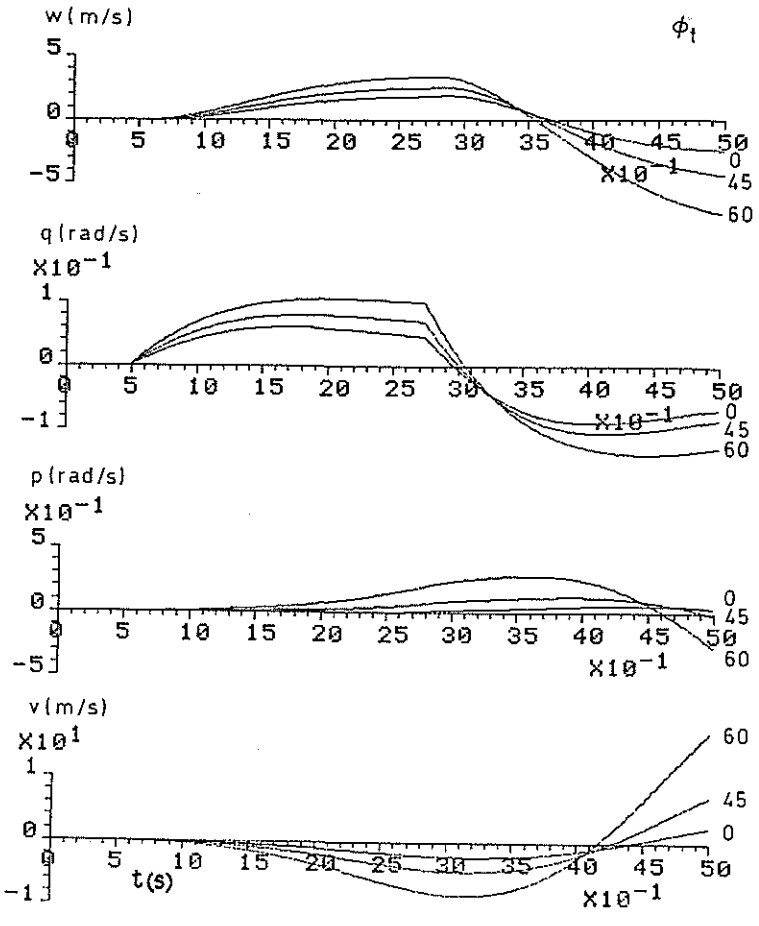

Fig 6 Short term response to longitudinal cyclic input, 100 kn

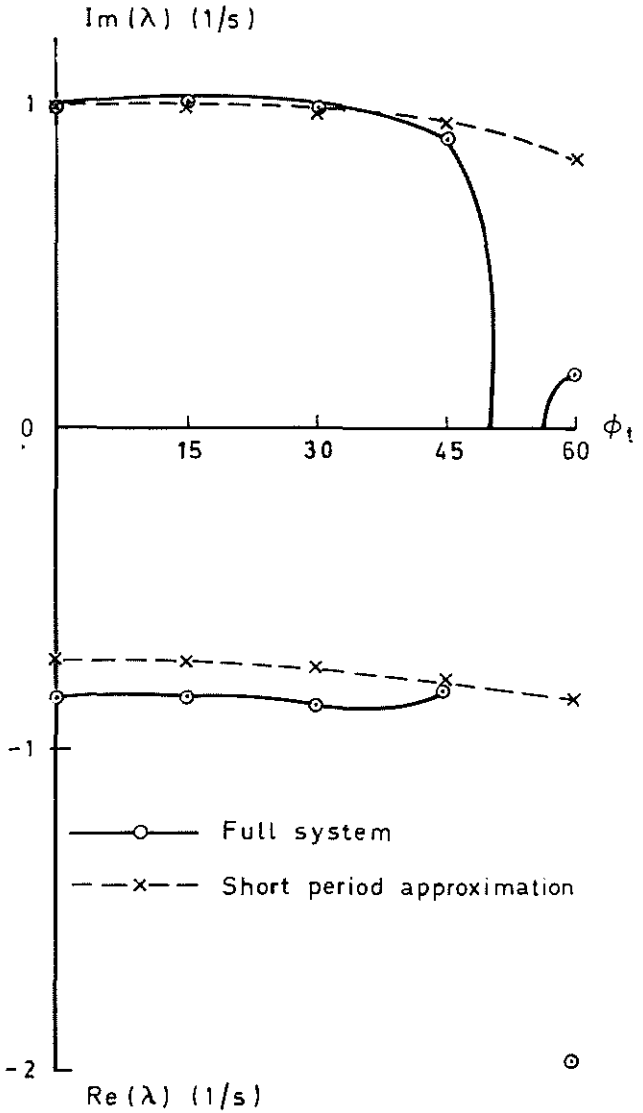

Fig 7 Stability diagram, 60 kn

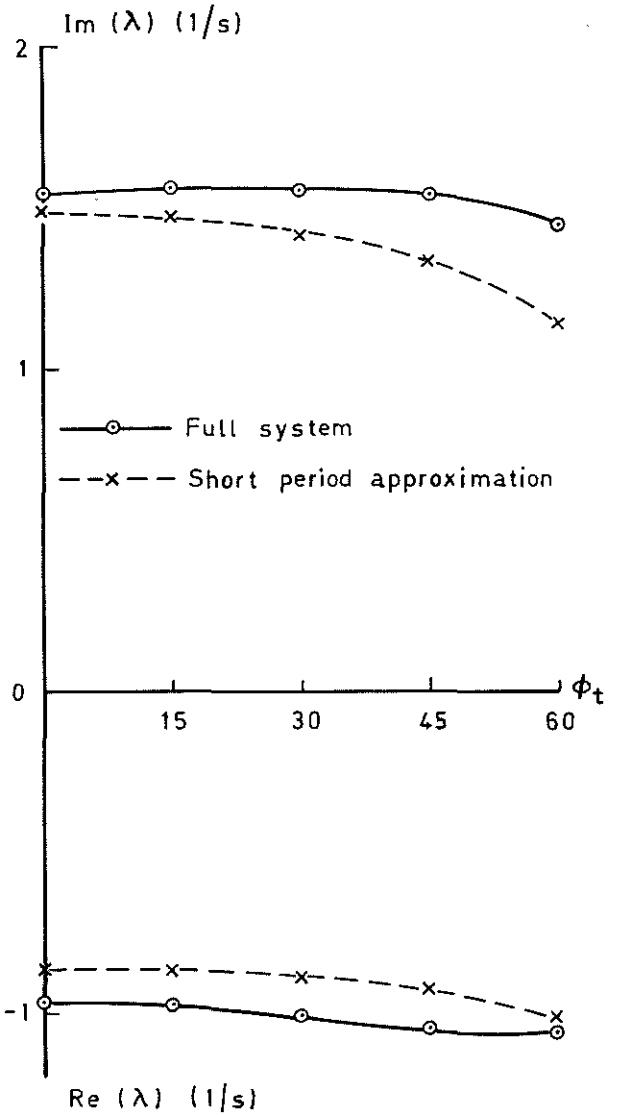

Fig 8 Stability diagram, 100 kn

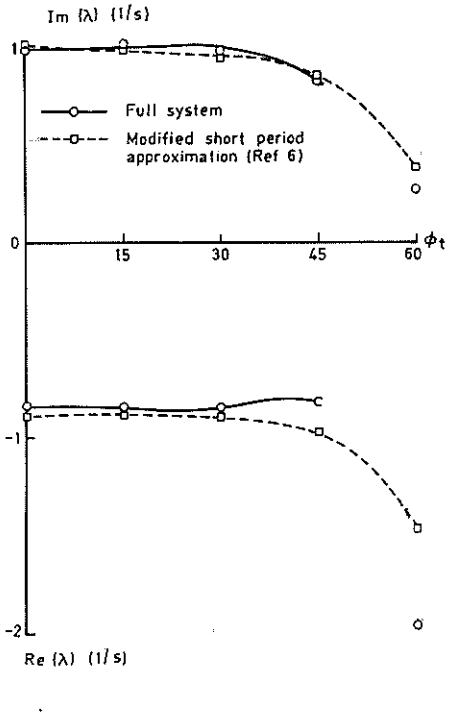

Fig 9 Stability diagram, 60 kn

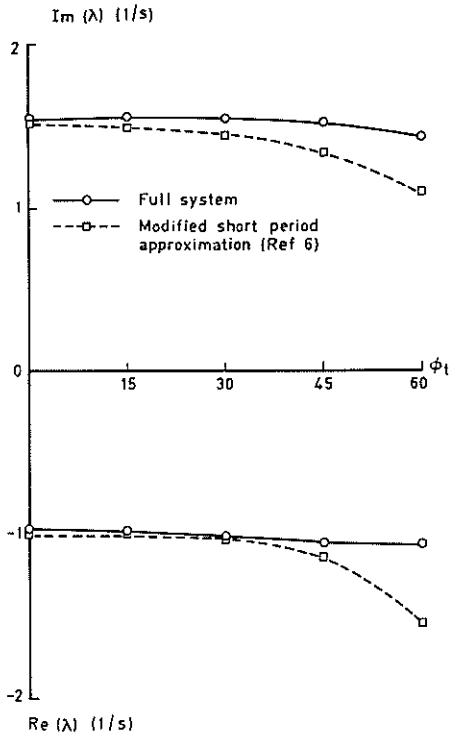

Fig 10 Stability diagram, 100 kn

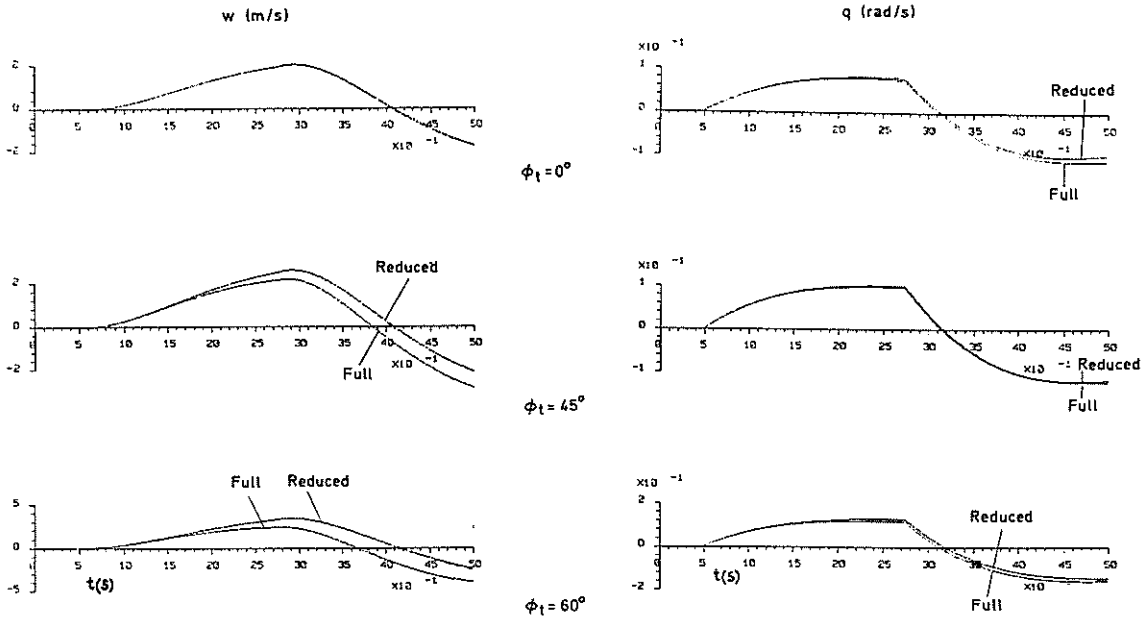

Fig 11 Longitudinal response, 60 kn - full system and eq (4)

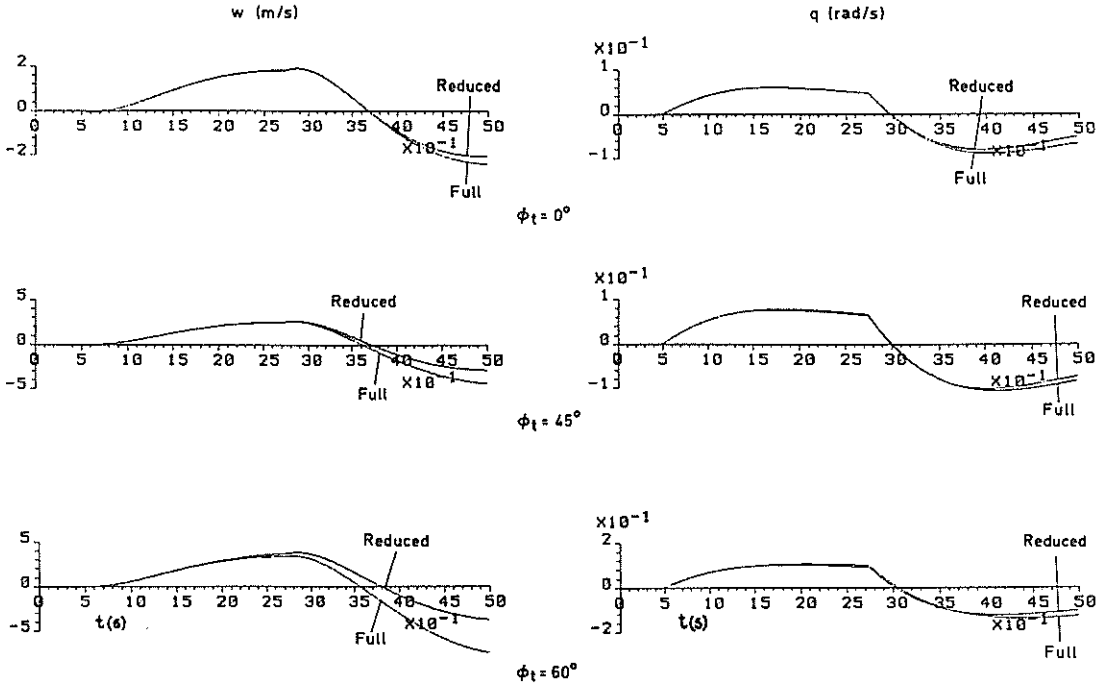

Fig 12 Longitudinal response, 100 kn - full system and equ (4)

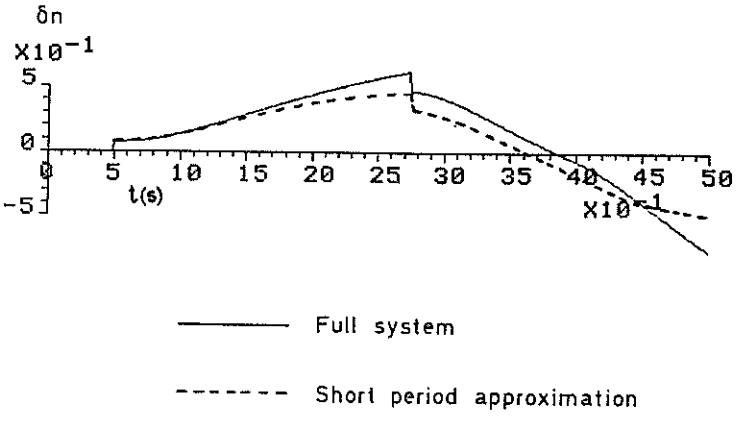

Fig 13 Normal acceleration, $\phi t = 60°$, 100 kn

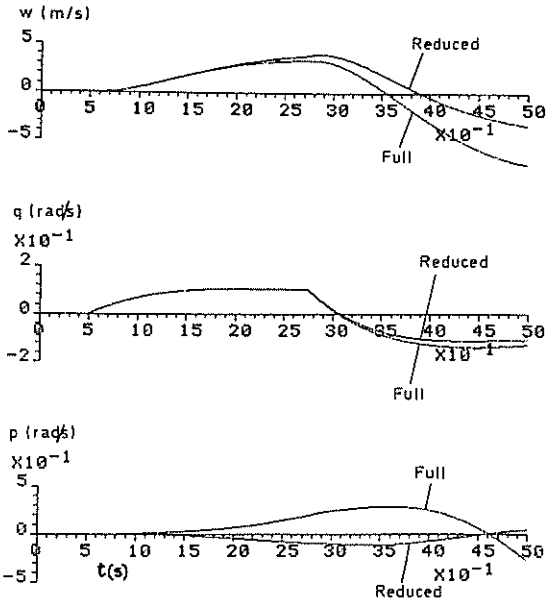

Fig 14 Longitudinal response, 100 kn - full system and eq (6)

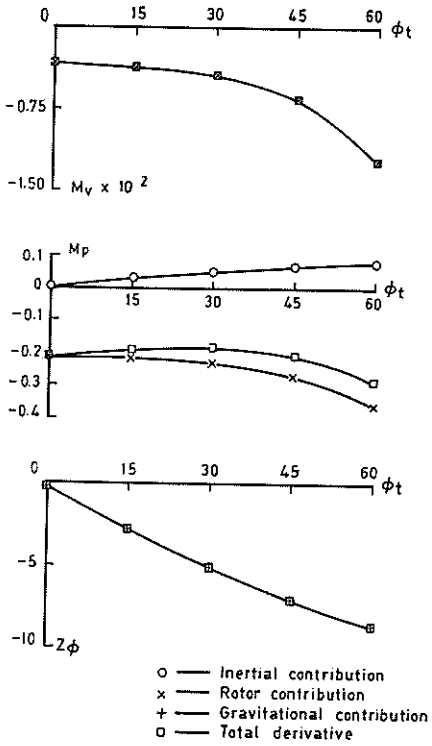

Fig 15 Breakdown of derivatives M_v , M_p and Z_ϕ , 100 kn

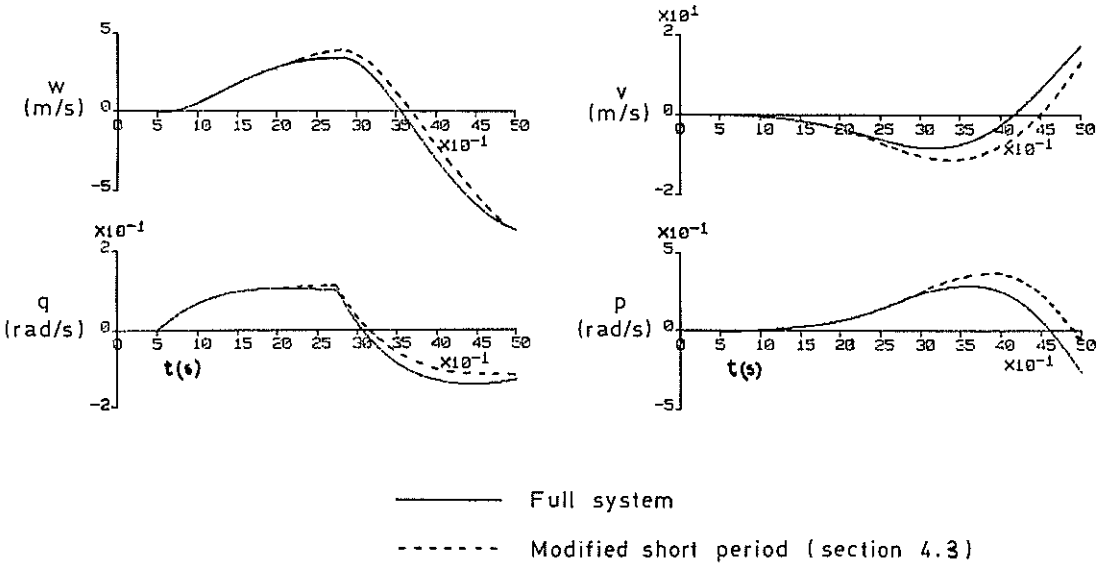

Fig 16 Modified short term response, $\phi_t = 60°$, 100 kn

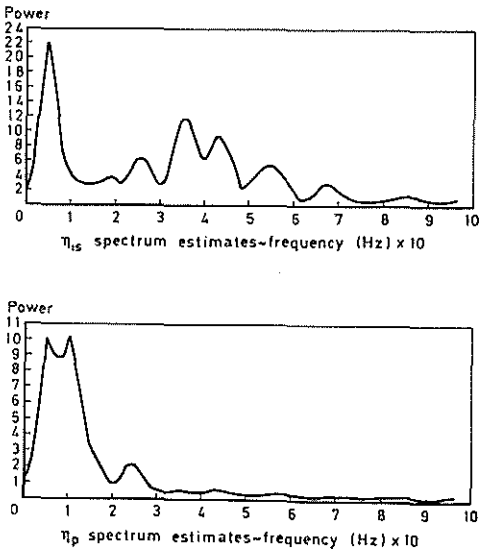

Fig 17 Power spectra for η_{ls} and η_p

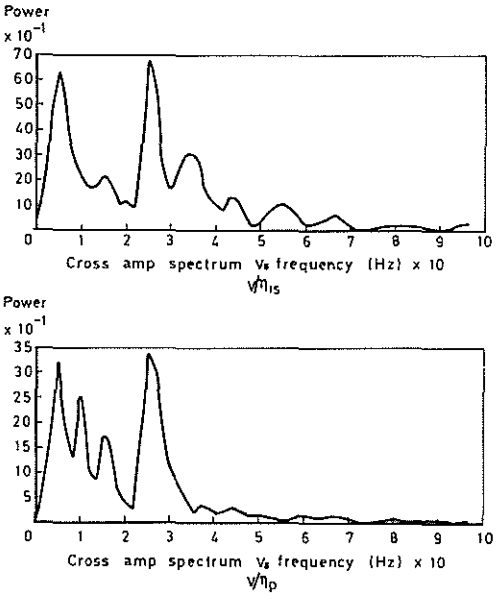

Fig 19 Cross amplitude spectra; v/η_{ls} , v/η_p

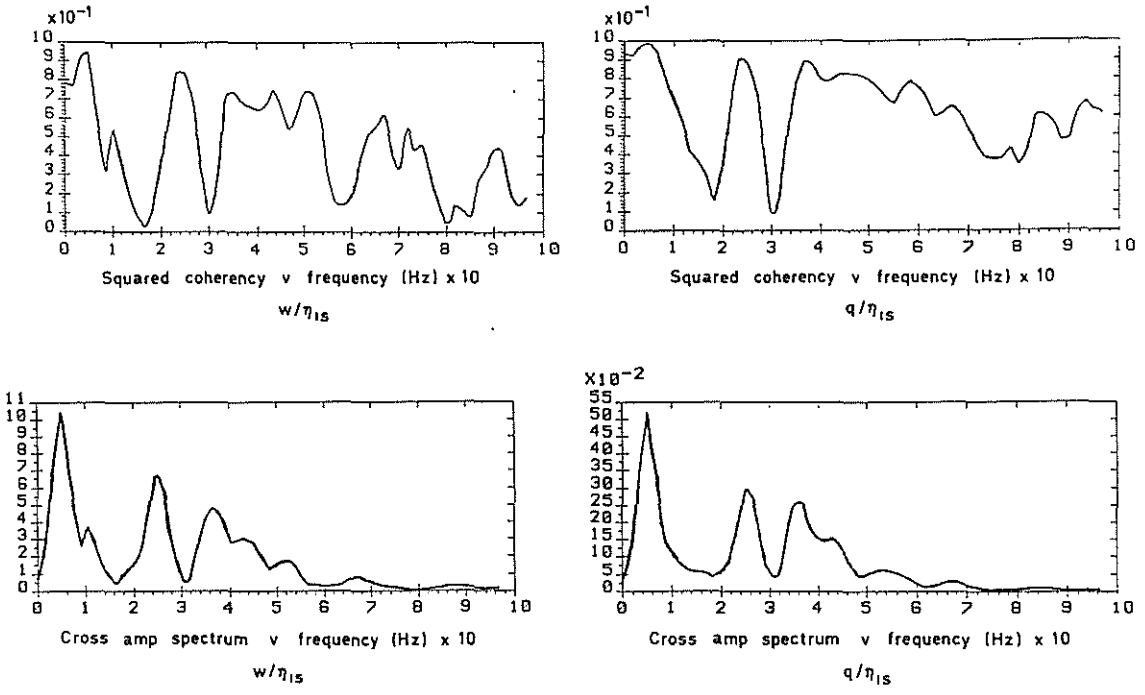

Fig 18 Coherency and cross amplitude spectra; w/η_{ls} , q/η_{ls}